THE ASTROPHYSICAL JOURNAL, 263:32–42, 1982 December 1

A SPECTROSCOPIC INVESTIGATION OF THE NEBULOSITY AROUND LOW-LUMINOSITY QUASARS

TODD A. BOROSON AND J. B. OKE
Palomar Observatory, California Institute of Technology
AND
RICHARD F. GREEN
Steward Observatory, University of Arizona
Received 1982 March 29; accepted 1982 June 2

ABSTRACT

Off-nuclear spectra have been obtained for a sample of 12 low-redshift optically selected QSOs. Simple techniques involving spectral differences between the nucleus and the nebulosity were used to effectively remove the scattered light. Ten of the 12 objects were found to be embedded in nebulosity dominated by starlight. Three of the objects show probable Mg I *b* λ5175 absorption, and one shows possible Hβ absorption. Mg I *b* absorption at a strength typical of an elliptical galaxy can be ruled out in two of the objects. The luminosities of these underlying galaxies, derived from models, are 1–2 mag below brightest cluster members. Arguments involving the central concentration of galaxies and the amount of gas required to produce the observed emission lines suggest that most of the underlying galaxies are spirals.

Subject headings: galaxies: nuclei — galaxies: stellar content — quasars

I. INTRODUCTION

Although QSOs have by definition a predominantly stellar appearance, the existence of nebulosity around some of them has been known for a long time (Matthews and Sandage 1963; Sandage and Miller 1966; Arp 1970; Kristian 1973). The faintness of this fuzz has, until recently, frustrated attempts to study it quantitatively, but its presence has stirred controversies over the classification of these objects and the relation between QSOs and the nuclei of galaxies (Kristian 1973; Arp 1970; Sandage and Miller 1966).

Kristian (1973) interpreted the presence or absence of nebulosity around a sample of QSOs in terms of underlying luminous galaxies. This approach has recently been taken an important step further by imaging studies of QSOs at high spatial resolution (Hawkins 1978; Hutchings *et al.* 1981; Hutchings *et al.* 1982; Wyckoff, Wehinger, and Gehren 1981; Malkan, Margon, and Chaisson 1982). These investigators have attempted to devise methods to measure small, low-surface-brightness departures from the point spread function of a stellar source. The consensus is that such departures exist in almost all low-redshift QSOs. The difficulty of separating the nuclear light from that of the nebulosity, however, has prevented much more than speculation on the detailed nature of the underlying extended material, although all these researchers claim that the observed properties are consistent with galaxies.

A positive identification, of course, requires spectroscopic observations. A few objects have been studied in this manner. Investigations of 4C 37.43 (Stockton 1976), 3C 249.1 (Richstone and Oke 1977), and 3C 273 (Wyckoff *et al.* 1980*a*) have revealed only emission lines arising in the fuzz. This was the case for 3C 48 also (Wampler *et al.* 1975), until recent work (Boroson and Oke 1982) discovered a continuum dominated by early type stars on both sides of the QSO. Other objects (3C 206, Wyckoff *et al.* 1980*b*; PHL 1070, Morton, Williams, and Green 1978; III Zw 2, Green, Williams, and Morton 1978) show evidence of presumably stellar continuum radiation in the fuzz, but uncertain spectral features prevent detailed analysis. Also, attempts to make the connection between galaxies and QSOs by looking for highly diluted stellar absorption lines in QSO spectra have not been successful (Miller, French, and Hawley 1980). These results should be contrasted with similar studies of N galaxies and BL Lac objects in which careful spectroscopic and photometric measurements have revealed evidence for the presence of an old stellar population (Sandage 1973; Thuan, Oke, and Gunn 1975; Miller, French, and Hawley 1979).

The most obvious remaining questions about the nebulosity and the connection between QSOs and galaxies are: (1) Are all QSOs in galaxies? (2) What is the luminosity function of the underlying galaxies, and is it related in some way to the luminosity of the QSO nuclei? (3) What are the morphological types of the underlying galaxies? (4) Why do QSOs form? Is their formation related in some way to a specific evolutionary or environmental event in the life of a galaxy?

In this paper we describe a study aimed at answering these questions by analyzing spectra of the fuzz around a sample of QSOs. The sample and observations are discussed in § II. The techniques by which total luminosities and the spectral appearance of the underlying galaxies are derived are explained in § III. The

implications of the findings, particularly with respect to the four questions above, are discussed in § IV. Section V summarizes our results.

II. THE SAMPLE AND THE OBSERVATIONS

There are two strong arguments in this type of investigation for choosing a sample carefully. First, the ambiguity between distant Seyfert galaxies and QSOs (which might have different properties) could result in a mix of objects. If one chose objects on the basis of known nebulosity, for instance, the sample might consist only of barely resolved Seyferts. Second, it is desirable to derive statistical properties such as the luminosity function and correlations between QSOs and fuzz, and these must be determined from complete samples free from confusing selection effects. Unfortunately, selection effects are inherent in the techniques used to discover quasars because of the ambiguity of the definition of a quasar and the overlap with other sorts of objects. Since there may or may not be a connection among all the active nuclear phenomena and QSOs, the most unbiased course would be to study a sample chosen only on the basis of activity in a group of extragalactic objects. The closest we can come to such a selection criterion with existing samples is to study objects chosen for their ultraviolet excess. This approach biases the sample *away* from objects in which an underlying galaxy produces a major fraction of the light, as that makes the integrated light too red for inclusion in the sample. The sample we chose to consider consists of all PG QSOs (Green and Schmidt 1982) with redshifts less than 0.20 and positions between 15^h and 1^h right ascension. A drawback of this particular sample is the low luminosity of most of the objects in it. Several of these "QSOs" are known to be extended and have been called N systems or Seyfert galaxies in previous studies. However, with the understanding that this sample should be biased neither toward nor away from any one type of UV excess object, we consider the properties of the sample as a whole to be representative of active extragalactic objects.

Fifteen objects fall into the category described above, and all but three were observed on the nights of 1981 July 9 through July 11 with the Double Spectrograph on the Hale 5 m telescope. The objects which were not observed are 1534+58, 1552+08, and 0026+12. At the time of the observations, only the blue camera of the Double Spectrograph had been completed. The detector used was a 320 by 512 pixel RCA charge coupled device (CCD). The grating which was used gave a spectral dispersion of about 2 Å per pixel and was set such that the region from 4700 to 5400 Å in the rest frame of each object was covered. The spatial scale on the detector was 0.″78 per pixel. A 2″ wide slit was used for all observations. Each object was observed twice, first with the slit centered on the nucleus (the nuclear spectrum), then with the slit offset by 2″ or 3″ (the nebular spectrum). This offset was made in the direction of the brightest part of the fuzz if any was visible on the screen of the acquisition television. The details of the observations are given in Table 1.

The data were reduced in two sequential steps, the first of which corrected the two-dimensional images and the second of which calibrated the one-dimensional spectra extracted from the two-dimensional images. The two-dimensional processing included subtraction of a bias level, which comes from the electronics and from a uniform low light level applied to the chip to reduce spreading due to charge transfer inefficiency. The images were then corrected for small-scale sensitivity variation. The sky spectrum was determined at each wavelength from an average of about 10 pixels on each side of the

TABLE 1

JOURNAL OF OBSERVATIONS

QSO	OTHER NAME	z	EXPOSURE TIME[a] (s)		POSITION OF NEBULOSITY SLIT	
			Nucleus	Nebulosity	Distance from Nucleus[b]	P.A. of Offset[c]
1501+10.....	...	0.037	750	2500	3	270
1519+22.....	...	0.136	750	2500	2	270
1535+54.....	I Zw 120	0.039	750	2500	3	330
1612+26.....	Ton 256	0.131	750	2500	2	270
1613+65.....	...	0.129	750	2500	2	270
1617+17.....	...	0.114	750	2500	2	270
1626+55.....	...	0.132	750	3000	2	270
2130+09.....	II Zw 136	0.063	750	2500	3	270
2209+18.....	II Zw 171	0.070	750	2500	2	270
0007+10.....	III Zw 2	0.090	750	2500	2	270
0049+17.....	...	0.064	750	2500	2	270
0052+25.....	...	0.154	750	2500	2	90

[a] Exposure time in seconds for observations of nucleus and nebulosity.

[b] Distance in arcseconds from center of nucleus to center of slit in exposure on nebulosity.

[c] Position angle in degrees at which slit was moved from nucleus for exposure on nebulosity. Length of slit was always oriented perpendicular to this angle.

spectrum and was subtracted from it. Then the one-dimensional spectra were extracted by adding consecutive rows in the image. The number of rows was chosen to maximize the signal-to-noise ratio. Comparison arc spectra were similarly flattened and collapsed to one dimension.

The one-dimensional comparison spectra were then fitted with cubic wavelength polynomials. The residual errors in the fits, which were typically to seven or eight lines, were never more than 0.10 Å. The spectra were corrected for atmospheric extinction and were calibrated approximately to absolute fluxes using observations of spectrophotometric standard stars obtained through apertures with 10″ diameters the same nights. Figures 1 and 2 show nuclear and nebular spectra for two of the objects observed.

III. ANALYSIS

As expected, a visual comparison of the nuclear and nebular spectra for each object shows that the contamination of the nebular spectrum by scattered light from the nucleus is a considerable problem. Most of the nebular spectra clearly show the broad Hβ emission which must arise only in the nucleus. What is desired is a method by which this scattered light can be subtracted, leaving only the spectrum intrinsic to the nebulosity. Unfortunately, because of refraction and scattering in the atmosphere and telescope, the scattered

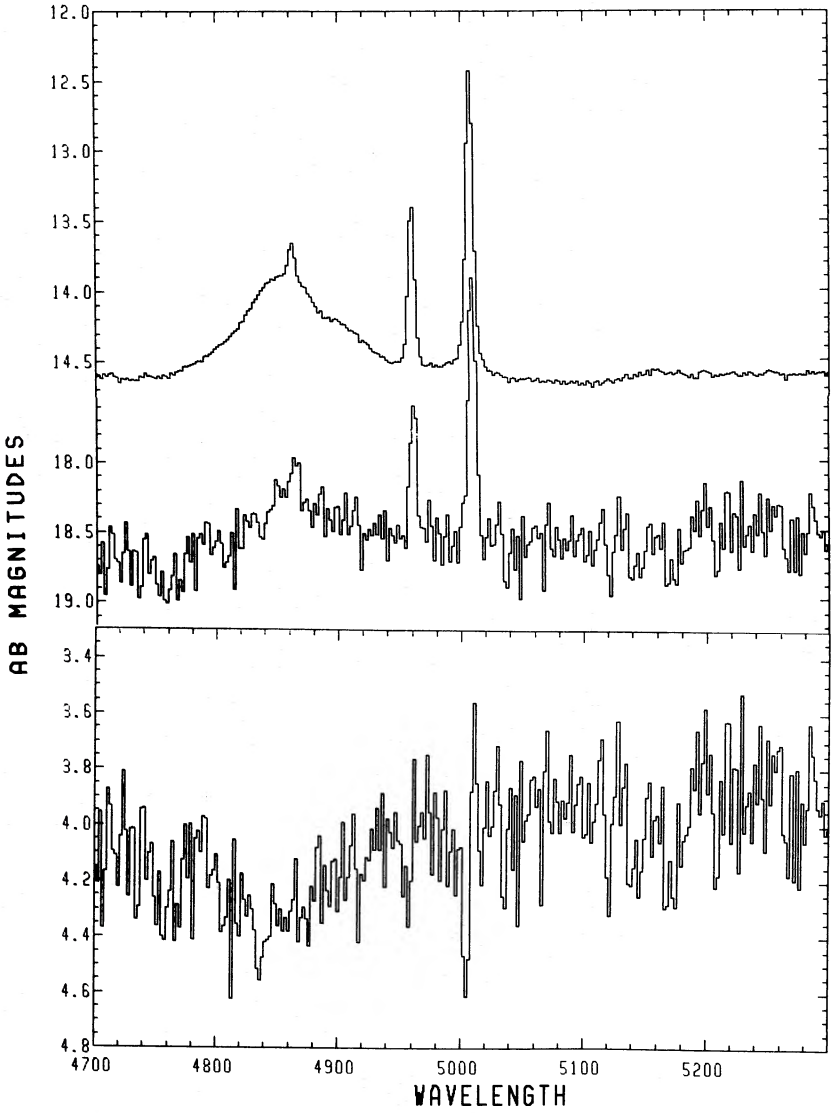

FIG. 1.—Nuclear (*top*) and nebular (*middle*) spectra in monochromatic magnitudes of the QSO 1501 + 10. Wavelengths have been converted to the object's rest frame. Hβ and the [O III] λλ4959, 5007 lines are the obvious emission features. The bottom spectrum is the ratio of the nebular to nuclear spectrum, also plotted in monochromatic magnitudes against rest wavelength. Note the broad Hβ "absorption" feature indicative of continuum radiation arising in the nebulosity and the weak Mg I *b* λ5175 absorption line.

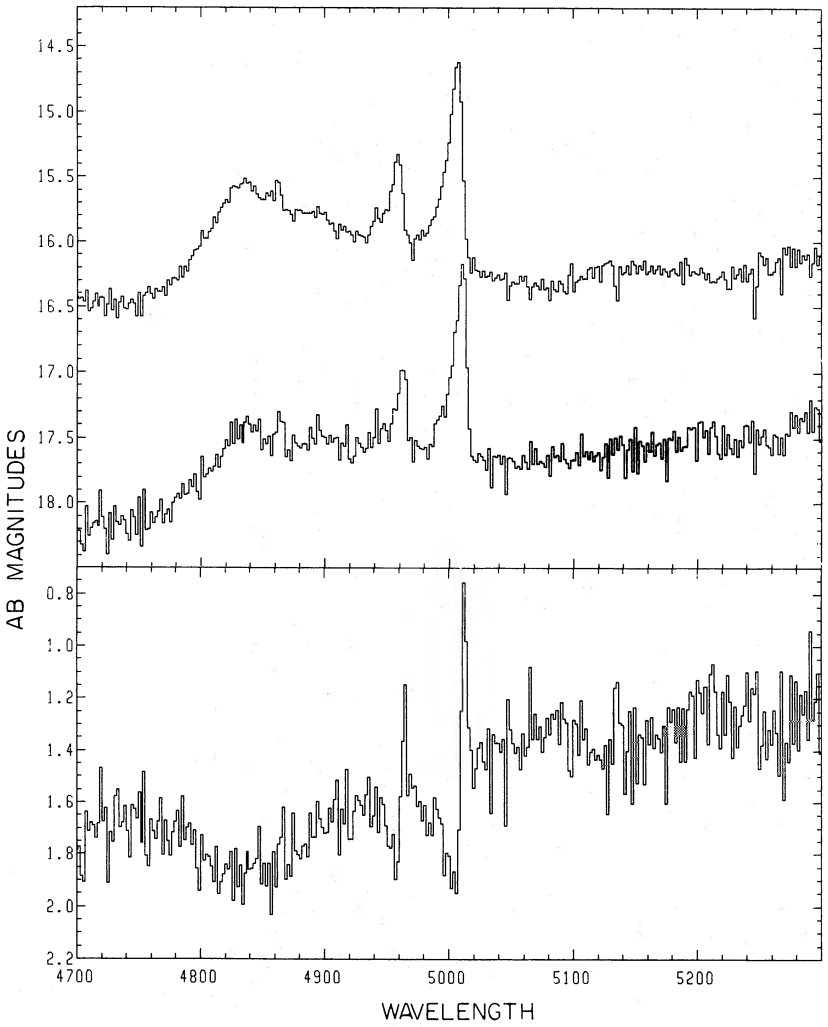

FIG. 2.—Nuclear (*top*) and nebular (*middle*) spectra of the QSO 0049+17 and their ratio (*bottom*). Note the asymmetric line profiles and the apparent shift in the [O III] line positions between nucleus and nebulosity.

light is a function of wavelength. Furthermore, because of seeing and guiding fluctuations, the relative amount of contamination varies from object to object.

The two aspects of the nebulosity we wish to investigate are the total luminosity and any indication of the nature of the emitting material. The first of these, the brightness of the fuzz, can be determined by a straightforward analysis. If we assume that the broad Hβ emission arises solely in the nucleus, then the ratio of the nebular spectrum to the nuclear spectrum will indicate whether any light from an underlying extended source is present. In the case that the light is all just scattered light, then the division will yield just the scattering spectrum, *which should be devoid of spectral features.* If, however, there is additional continuum present in the nebulosity, the ratio will show a broad Hβ "absorption" feature. Moreover, the strength of this "absorption" feature, compared to the strength of the Hβ emission line in the nuclear spectrum, can be used to determine the fraction of the nuclear light which has been scattered into the nebular slit. This relation is due to the difference in the equivalent width of Hβ between the nucleus and the fuzz. Specifically, if one measures the intensities at the line center and in the continuum interpolated to the position of the line center (denoted Q_l and Q_c for the nuclear spectrum, R_l and R_c for the ratio), it can be shown that the intrinsic fuzz intensity in the continuum at the position of Hβ is

$$F = \frac{Q_l Q_c}{Q_l - Q_c}(R_c - R_l) .$$

This division was performed for the pair of spectra of each object, and the divided spectra for two of the objects are shown in Figures 1 and 2. With the exception of two objects, 1612+26 and 1617+17, all of these clearly show the broad Hβ "absorption" feature indicative of the presence of continuum in the nebulosity. The

intensities described above were measured and the galaxy brightness in the off-nuclear slit was calculated for each object. For the two cases which do not show the obvious broad absorption, upper limits on the brightness of the galaxies were derived. These magnitudes are given in Table 2 along with the corresponding apparent and absolute magnitudes of the nucleus. All magnitudes refer to the *continuum* at 4861 Å in the rest frame of the object, and all units are *AB* magnitudes ($AB = -2.5 \log f_{\rm nu} + 48.60$, where $f_{\rm nu}$ is the flux in ergs s^{-1} cm^{-2} Hz^{-1} [Oke 1965*b*; Oke and Gunn 1982]). As a check on this technique a bright star was observed and reduced in the same manner. There appeared to be no difference in the equivalent width of its absorption lines between the on-center and off-center spectra; and their ratio, aside from a "P Cygni–like" spike caused by a slight wavelength shift, was featureless.

The next step in the analysis is to calculate, from the measured magnitude in each off-nuclear slit, the total magnitude of the underlying galaxy. We have done this in two different ways. First, we have used a very conservative approach, which undoubtedly yields a lower limit to the total galaxy luminosity. This is to divide the observed luminosity by a factor roughly indicative of the fraction of the total galaxy we have observed in our slit. The factor used was 1/4 for those observations centered 2″ from the nucleus and 1/6 for those centered 3″ from the nucleus. The total absolute magnitudes for the underlying galaxies, derived in this manner, are given in column (6) of Table 2.

The other technique used to determine total luminosities was to construct models of the light distribution of the underlying galaxies. These models consisted of an exponential disk for spirals (Freeman 1970; Boroson 1981) or a de Vaucouleurs $r^{1/4}$ law (de Vaucouleurs 1948) for ellipticals. For each QSO a sequence of spirals and a sequence of ellipticals with different scale lengths were considered. Given the redshift and off-nuclear slit position and area for that object, the intensity of the galaxy was calculated. Then the surface brightness parameter was adjusted to match the observed magnitude. Thus, each model generated a point in the log scale length—surface brightness plane [$\log \alpha^{-1}$ vs. $B(0)_c$ in the notation of Freeman 1970 for spirals, $\log r_e$ vs. B_e in the notation of de Vaucouleurs 1953 for ellipticals]. The lines which connect these points define the locus on which all suitable models must lie. Figure 3 shows the log scale length versus surface brightness diagram with the tracks for three of the objects.

Two other constraints are applicable to this calculation. We have limited the allowed ranges of the scale lengths and surface brightness parameters to the values seen in normal galaxies. For spirals we consider exponential scale lengths, α^{-1}, between $1\frac{1}{2}$ and 10 kpc and central surface brightness, $B(0)_c$, between 20 and 24 mag $arcsec^{-2}$ (Boroson 1981). For ellipticals we consider effective radii r_e between 1 and 12 kpc and effective surface brightnesses B_e between 20 and 23.5 mag $arcsec^{-2}$ (Kormendy 1977). A Hubble constant of 50 km s^{-1} Mpc^{-1} was used in all calculations. The differences between our magnitudes, measured at 4861 Å, and the usual *B* magnitudes was ignored for the purpose of defining these limits.

The other constraint on the underlying galaxies is obtained from the nuclear spectra. If the galaxy is an elliptical, in which case we assume the stellar population has a late spectral type, the Mg I *b* λ5175 absorption

TABLE 2

MAGNITUDES OF THE UNDERLYING GALAXIES

QSO (1)	Slit Area (2)	m_Q (3)	m_G (4)	M_Q (5)	M_G (min) (6)	$-M_G$ (spiral) (7)	$-M_G$ (ell.) (8)	L_Q/L_G (9)
1501+10	8.1	14.63	19.07	−22.1	−19.6	20.3–22.2	21.2–21.4	2.2
1519+22	5.8	16.64	19.73	−22.9	−21.4	21.9–22.5	...	1.6
1535+54	7.0	15.05	19.44	−21.8	−19.4	20.0–21.8	20.9–21.0	2.2
1612+26	4.6	16.50	20.40	−23.0	−20.6	21.3–22.0	21.9–22.0	3.4
1613+65	4.6	16.45	18.99	−23.0	−22.0	23.4–23.5	...	0.6
1617+17	4.6	16.33	20.40	−22.8	−20.3	21.0–21.9	21.6–21.7	3.6
1626+55	4.6	16.90	19.11	−22.6	−21.9	23.0–23.3	...	0.5
2130+09	10.4	15.60	19.62	−22.3	−20.2	20.8–21.8	21.4–21.6	2.5
2209+18	10.4	16.30	18.57	−21.8	−21.0	21.6–22.6	22.1–22.3	0.6
0007+10	9.3	15.82	19.46	−22.8	−20.7	21.0–22.1	21.8–21.9	2.9
0049+17	8.1	16.56	19.98	−21.4	−19.5	19.9–21.6	20.5–20.8	1.7
0052+25	8.1	16.15	19.93	−23.7	−21.4	21.8–22.2	22.4–22.6	4.4

NOTE.—Col. (1), name of object. Col. (2), area of slit used for nebulosity in $arcsec^2$. Col. (3), observed apparent monochromatic magnitude of nucleus at λ4861 in the rest frame of the object. Col. (4), observed apparent monochromatic magnitude of nebulosity (corrected for scattered light) at λ4861 in the rest frame of the object. Col. (5), absolute magnitude of the nucleus at λ4861 in the rest frame of the object. Col. (6), conservative lower limit to the absolute magnitude of the total underlying galaxy (the galaxy must be brighter than this). Col. (7), range of acceptable absolute magnitudes of total underlying galaxy based on models of spirals. Note change in sign. Col. (8), range of acceptable absolute magnitudes of total underlying galaxy based on models of spirals. Note change in sign. Col. (9), ratio of nuclear luminosity to luminosity of underlying galaxy at λ4861 in the rest frame of the object.

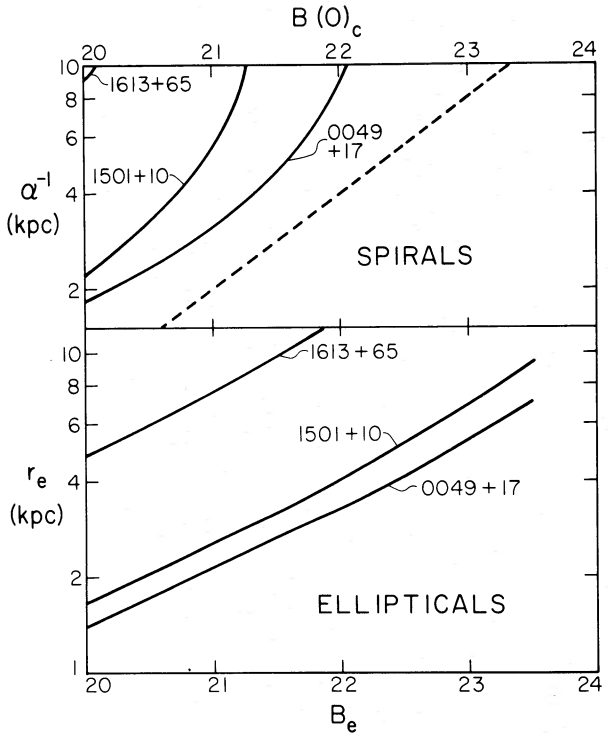

FIG. 3.—The log scale length vs. surface brightness diagrams for spiral and elliptical galaxies. Tracks for three of the underlying galaxies are displayed. A line of constant luminosity is shown as a dashed line.

feature should be visible in the nuclear spectrum. This actually provides a fairly powerful discriminant between elliptical galaxies which are quite centrally concentrated and spirals which are not. The Mg I *b* feature is not convincingly seen in any of the nuclear spectra, and so a limit can be placed on the central surface brightness of an underlying elliptical galaxy. This limit has been used to further reduce the region in which the parameters are allowed. In three cases, 1613+65, 1626+55, and 1519+22, the locus of permitting points in the (log r_e, B_e)-diagram is completely excluded by this central surface brightness constraint. These underlying galaxies cannot be as concentrally concentrated as an elliptical galaxy and still produce the observed off-nuclear intensity. Thus, in these three cases, only spiral galaxy luminosity distributions are consistent with the observed brightnesses.

The final step is to determine the total luminosities of the allowed models. In the (log scale length, surface brightness)-diagram, lines of constant luminosity have slope 5 and so are remarkably similar to our tracks of allowed models. The result of this is that although allowed models may have very different parameters, their total luminosities will be quite similar. A line of constant total luminosity is shown as a dashed line in Figure 3. Table 2 lists, for each QSO, the range of total luminosity (obtained by integrating the surface brightness law out to infinity) for both spiral and elliptical models.

The other information we would like to derive from the spectra is some indication of the detailed nature of the emitting material. The ratio procedure used to determine the magnitudes of the underlying galaxies is sensitive only to the continuum. The strengths of emission and absorption features in each nebular spectrum would provide information on the relative contributions of gas and stars to the continuum and on the age of the stellar population. These quantities are the only spectroscopic handle on the morphological type of the underlying galaxies and the effects of the QSOs on them. Using the amount of contamination by the nuclear spectrum derived from the ratio analysis, we were able to remove the scattered light from each nebular spectrum. These spectra, therefore, show the intrinsic features of the nebulosity only. They are presented in Figure 4.

It is obvious, from the spectra shown in Figure 4, that the light in almost all of the objects is dominated by continuous radiation; emission lines contribute only a small fraction of the total flux. Although at first glance the spectra of the nebulosity show no obvious signs of absorption lines, three of the objects, 1501+10, 1535+54, and 2209+18, have depressions in the continuum level at the position of Mg I *b* (λ5175). Although we cannot positively ascertain the reality of this identification, the observed strengths are typical of old stellar populations, and we believe that the lines are probably there. The QSO 1626+55 shows a similarly marginal absorption line at the position of Hβ (λ4861). In all but one of the objects there is some line emission present. The fluxes of the emission lines seen and the equivalent width of the [O III] λ5007 line are given in Table 3. Note that these fluxes apply to the apertures whose areas are listed in Table 2.

IV. DISCUSSION

a) Are all QSOs in Galaxies?

Recent work has shown that most if not all low-redshift QSOs reside in extended, low-surface-brightness nebulosity (Wyckoff, Wehinger, and Gehren 1981; Hutchings *et al.* 1982; Malkan, Margon, and Chaisson 1982). Previous spectroscopic investigations, however, have turned up only emission lines in the fuzz in many cases (Wampler *et al.* 1975; Stockton 1976; Richstone and Oke 1977; Wyckoff *et al.* 1980*a*), suggesting that, in these objects, the nebulosity may be merely clouds of gas ionized by the QSO. Several objects do show continuum in the fuzz (Wyckoff *et al.* 1980*b*; Morton, Williams, and Green 1978; Green, Williams, and Morton 1978; Boroson and Oke 1982); these objects are in general of lower luminosity than those which show only emission lines.

We have found that in 10 of the 12 objects in our sample most of the light from the extended nebulosity is continuum radiation. The possibility that this continuum is bound-free and free-free hydrogen emission can be ruled out because at all reasonable temperatures the equivalent width of Hβ would be 100 Å or larger

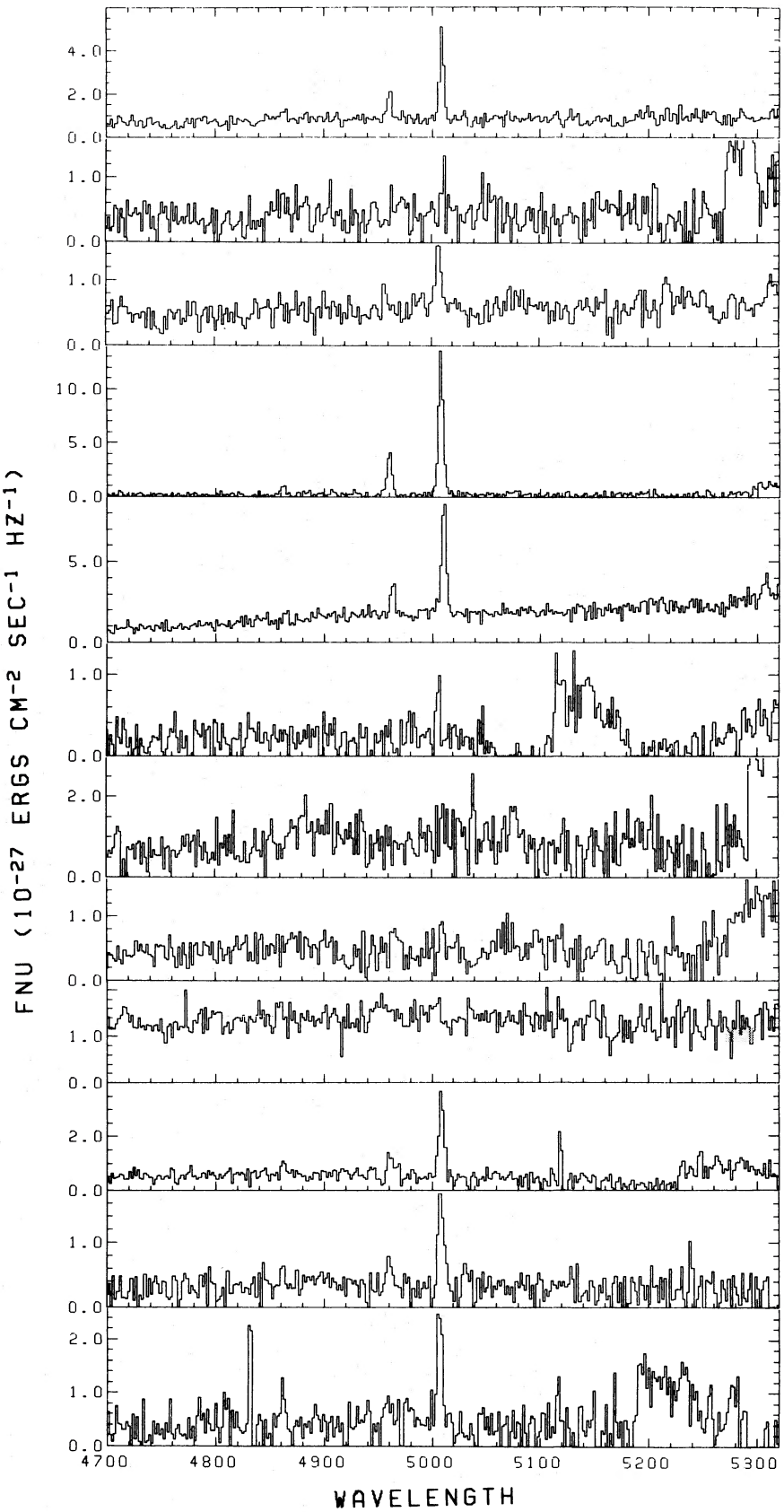

FIG. 4.—Spectra of the nebulosity around the QSOs (from top to bottom) 1501+10, 1519+22, 1535+54, 1612+26, 1613+65, 1617+17, 1626+55, 2130+09, 2209+18, 0007+10, 0049+17, and 0052+25. Contamination from the QSOs has been removed. Wavelengths have been converted to the rest frame of the respective objects. The broad dips and bumps seen on the red sides of several of the spectra (particularly 1519+22, 1617+17, 1626+55, 2130+09, 0007+10, and 0052+25) are due to a defect in the detector which was discovered after the observations were completed.

TABLE 3

EMISSION LINE FLUXES IN NEBULOSITY[a]

QSO	Continuum Detected?	Hβ	[O III] λ4959	[O III] λ5007	[O III] λ5007 E.W.[b]	Comments
1501+10	Yes	3.3	8.1	24.0	25	Mg I *b*?
1519+22	Yes	<2.0	<2.0	4.2	9	
1535+54	Yes	<2.0	2.0	8.6	13	Mg I *b*?
1612+26	No	7.1	35.0	90.0	...	
1613+65	Yes	3.8	12.0	50.0	23	
1617+17	No	<3.0	<3.0	5.8	...	Bad at $\lambda > 5050$
1626+55	Yes	<5.0	<5.0	<5.0	...	Hβ abs?
2130+09	Yes	<2.0	2.9	2.5	4	
2209+18	Yes	2.0	<2.0	1.8	1	Mg I *b*?
0007+10	Yes	4.3	7.8	23.0	38	Bad at $\lambda > 5220$
0049+17	Yes	1.6	3.4	11.0	31	
0052+25	Yes	4.9	3.4	16.0	27	Bad at $\lambda > 5180$

[a] Fluxes in units of 10^{-16} ergs cm^{-2} s^{-1}. Uncertainties are about 2 in these units.
[b] Equivalent width of [O III] λ5007 in angstroms.

(about 100 Å at 160,000 K, rising to 600 Å at 10,000 K [Oke 1965*a*]). Since the observed Hβ equivalent widths are in all cases at least an order of magnitude smaller than this, the source of the continuum must be stars. Thus, we conclude that in these 10 objects the QSO really is embedded in a galaxy. The two objects in which we were unable to detect a continuum both show emission lines (as do nine out of 10 of the other objects). In 1617+17 all we can claim with certainty is the presence of an [O III] λ5007 line. In 1612+26, however, quite strong emission is visible in both [O III] lines and Hβ. Our findings support those of the various imaging studies: all low-redshift QSOs are embedded in nebulosity of some sort. Furthermore, starlight is the dominant source of emission in at least 10 of the 12 objects. Further observations of 1612+26 and 1617+17 are required to determine whether these objects are actually different from the rest of the sample.

The limitations of the sample are quite important in the context of statistical analysis of the properties of the fuzz. Although it is almost complete in the sense that a distance-limited sample has been drawn from a magnitude-limited sample, it is clear that high-luminosity objects ($M < -24$ mag) are not represented, and a strong correlation between redshift and luminosity indicates that a Malmquist bias is present. Therefore, we hesitate to draw any conclusions about the properties of QSOs in general from this sample. We do point out that the range of luminosities represented in this sample overlaps the lower part of the range studied by Wyckoff, Wehinger, and Gehren (1981) and Hutchings *et al.* (1982).

b) The Luminosities of the Underlying Galaxies

Figure 5 shows the ranges of total luminosity found for the 12 underlying galaxies, plotted against the luminosities of the QSOs. At the bottom of Figure 5 are plotted estimates from Wyckoff, Wehinger, and Gehren (1981) of the ranges of luminosity observed for several types of galaxies. Included in this compilation are nearby spirals, nearby ellipticals, brightest cluster members, Seyfert galaxies, N galaxies, the underlying galaxies in BL Lac objects, and the underlying galaxies in QSOs as determined by Wyckoff *et al.* Their tabulated values for all of these samples have been corrected to our adopted distance scale and magnitude system. Again we find agreement with previous imaging studies. The luminosities of the underlying galaxies are in the

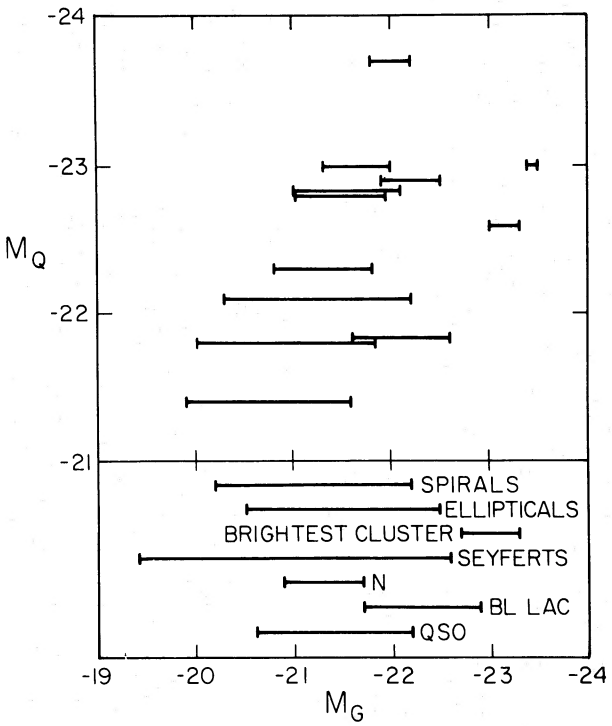

FIG. 5.—*Top*, a plot of the luminosities of the central QSOs against the total luminosities of the underlying galaxies. *Bottom*, the ranges of luminosities of galaxies of various types (from Wyckoff *et al.* 1981) in the same magnitude system. The ranges labeled N, BL Lac, and QSO refer to the underlying galaxies only in these types of systems.

range of moderately bright systems, but usually 1–2 mag fainter than brightest cluster galaxies. This result is encouraging, as these estimates of total luminosities have been derived in completely different ways.

There are several potential uncertainties in the derivation of the total luminosities. The imaging schemes require the subtraction of the point spread function of the nucleus, and this contains a contribution from the underlying galaxy which varies with redshift and seeing. Thus, an empirical correction must be applied (Hutchings *et al.* 1982) to recover this lost luminosity. Our technique has the inherent advantage that the contamination by scattered light is measured using the spectral differences between nucleus and nebulosity. The spectroscopic technique has the disadvantage, however, that the conversion from measured magnitude in an off-nuclear slit to the total luminosity of the underlying galaxy requires the many questionable assumptions which make up the model. In particular, we have assumed that the underlying galaxies are face-on and round, that they are well described by either a radial exponential or a de Vaucouleurs law, and that the observed parameters of these functions fall into the range of normal galaxies. Because we really do not know the properties of these systems, any or all of these assumptions could be in error.

A more fundamental error arises because of the unknown stellar population in these objects. When we compare luminosities, the quantity we are really trying to compare is mass. For elliptical galaxies, the luminosity is closely related to the mass; i.e., the mass-to-light ratio M/L does not vary very grossly among objects. If QSOs are associated with galaxies which are undergoing star formation (Boroson and Oke 1982), the M/L may be as much as a factor 10 lower than in an elliptical galaxy (Larson and Tinsley 1978). Under these circumstances the galaxy in question could be 2–3 mag brighter than an elliptical galaxy with the same mass. It is clear that before meaningful comparisons can be made between the underlying galaxies in QSOs and other types of galaxies, we must learn more about the stellar populations.

Perhaps slightly less dangerous comparisons can be made *among* the underlying galaxies. Figure 5 shows a possible correlation between M_G and M_Q significant at the 2 σ level. Note that the lower right corner of the diagram is not allowed, as objects here would be so galaxy dominated they would not have appeared stellar enough to be included in the sample. Objects in the sample could fall in the upper left corner, however; but, aside from the two upper limits, they seem to avoid that region. If real, this trend might indicate an inability for a luminous QSO to form in an intrinsically faint galaxy. Again, further observations of 1612+26 and 1617+17 are required to strengthen this conclusion.

c) *The Morphological Types of the Underlying Galaxies*

The question of whether QSOs occur in elliptical galaxies, spiral galaxies, or both is another which is plagued by selection effects. It is well established that active nuclei can occur in both major morphological types: in spirals as Seyferts (Adams 1977) and in ellipticals as radio galaxies or N galaxies (Sandage 1973; Miller, French, and Hawley 1980). Thus, to the extent that the sample is made up of unresolved systems of each of these types, the underlying galaxies will reflect this. The question is whether the ratio L_Q/L_G is distributed similarly for both morphological types. Are the objects which would appear stellar even at small distances in elliptical or spiral galaxies?

In order to answer this question properly we must first examine the measurable spectral quantities and how they can be used to distinguish the morphological types. We begin by mentioning the central surface brightness difference described in § III. Since ellipticals have a much higher degree of central concentration than spirals, an off-nuclear detection of starlight in an elliptical galaxy often implies that stars should be detected in the nucleus as well. Also, since ellipticals are known to generally consist of old stars only, the metal lines, which should be free of the complicating hydrogen emission lines, are the features of interest. This line of reasoning was followed by Miller, French, and Hawley (1980), who found no evidence for the presence of weak stellar absorption features in nine QSOs. Similarly, in three of the 12 objects in our sample we can rule out elliptical galaxies because an elliptical of sufficient luminosity to be seen in our off-nuclear slit at the observed magnitude would be easily visible in the nuclear spectrum. Table 2 shows, however, that these objects are three of the four with the smallest ratio L_Q/L_G.

Two aspects of the spectral appearance of the nebulosity suggest (but do not demand) that the underlying galaxies are mostly spirals. First, the existence of [O III] λ5007 emission in 11 of the 12 objects requires the presence of gas. The precise amount of gas is uncertain because no density-sensitive features are in the observed spectral range. The luminosities of the λ5007 emission range from 5×10^{39} ergs s^{-1} to 7×10^{41} ergs s^{-1}. Assuming a temperature of 12,500 K and a relative abundance $O^{++}/H = 4 \times 10^{-4}$ (following Bergeron 1976), these luminosities correspond to total masses of gas from $6 \times 10^7 (N_e)^{-1}\ M_\odot$ to $8 \times 10^9 (N_e)^{-1}\ M_\odot$. Reasonable guesses at N_e might be 100–1000 cm^{-3}, and the masses should be multiplied by a factor of about 10 because only about 10% of each underlying galaxy is observed with the off-nuclear aperture. Thus, typical gas masses in the underlying galaxies range from 10^6 to $10^8\ M_\odot$ if these assumed parameters are correct. For comparison, two techniques have been used to deduce the mass of gas in elliptical galaxies. Neutral hydrogen masses are calculated from measurements of 21 cm emission, and a recent compilation (Sanders 1980) indicates that about half of all well observed ellipticals have less than $10^8\ M_\odot$ of neutral hydrogen. Most of the observed ellipticals, however, have only upper limits determined, so the actual gas masses might be considerably less than this value in almost all cases. The second handle on the mass of gas in elliptical

galaxies comes from emission line fluxes. Osterbrock (1960) found that the mass of ionized gas in the nucleus of NGC 4278, a normal elliptical galaxy, is between 10^4 and 10^6 $M_\odot$, depending on the electron density. Unfortunately, very few elliptical galaxies have had their emission line fluxes measured, and such measurements are aplicable to only the *ionized* gas. Thus, the presence of gas in the underlying galaxies of QSOs is not truly inconsistent with what is currently known about ellipticals but is certainly more suggestive of spirals which are known to have larger gas masses.

The second feature of the spectra which is suggestive of spiral galaxies is the absence of strong Mg I *b* λ5175 absorption. This feature is one of the strongest in old stellar populations in the optical spectral range and typically has an equivalent width of 4–5 Å (Spinrad and Taylor 1971). It is probably present in three of the nebular spectra, 1501+10, 1535+54, and 2209+18. Two of the other spectra, however, 1519+22 and 1613+65, which have sufficiently large signal-to-noise ratios to easily see this feature, do not show it. The spectra of the remaining objects are too noisy to put interesting limits on its strength. If the underlying galaxies are spirals, more likely to be dominated by younger stars, the Mg I *b* absorption would be weaker or perhaps even absent.

d) QSOs and the Normal Evolution of Galaxies

We conclude the discussion with some speculation on how the formation and fuelling of QSOs as galactic nuclei fit into the picture of the evolution of galaxies. Stockton (1982) has pointed out that the density and luminosity evolution seen in QSO statistics is likely to be a result of QSO fuel sources drying up. Thus, the existence of QSOs at low redshifts might be explained by episodes in which a latent active nucleus is fueled by an encounter with another galaxy. In association with this idea, we note that such encounters between galaxies are known to result in bursts of star formation and bluer than normal colors in the participating objects (Larson and Tinsley 1978). Therefore, it might be expected that the underlying galaxies in low-redshift QSOs would show signs of recent star formation such as blue colors, high luminosities, and early type spectra. Although the evidence at present is meager, it is interesting that the underlying galaxy in 3C 48 has a mean spectral type of A7 (Boroson and Oke 1982) and that the objects studied here show some tendency toward early spectral type. We offer the suggestion that future studies of the spectral properties of the underlying galaxies in QSOs should be designed to be sensitive to hotter stars than are typical in giant elliptical galaxies.

V. CONCLUSIONS

We have obtained spectra of the nebulosity associated with 12 low-redshift QSOs. Ten of these objects are emitting most of their luminosity in continuum emission; the other two have only emission lines detectable at the level of sensitivity achieved in this study. The continuum comes from starlight, indicating that these QSOs are embedded in galaxies. The luminosities found for the underlying galaxies are consistent with the results of recent imaging studies of low-redshift QSOs: they are 1–2 mag fainter than the brightest galaxies in clusters. Several lines of reasoning suggest that the underlying galaxies are mostly spirals, but this result should be viewed with caution as it depends on many uncertain assumptions. Also, this conclusion applies only to fairly low luminosity QSOs, by which this sample is dominated. Finally, we note that there are reasons involving the fueling of low-redshift QSOs to expect the underlying galaxies to have young stellar populations.

We would like to thank F. Harris, G. Pauls, and B. Zimmerman for heroic hardware and software efforts, and J. Carrasco for able and jovial assistance at the telescope. One of us (T.A.B.) is pleased to acknowledge helpful discussions with A. Sandage, M. Malkan, and D. Schneider. This work was partially supported by the National Aeronautics and Space Administration through grant NGC-05-002-134.

REFERENCES

Adams, T. F. 1977, *Ap. J. Suppl.*, **33**, 19.
Arp, H. C. 1970, *Ap. J.*, **162**, 811.
Bergeron, J. 1976, *Ap. J.*, **210**, 287.
Boroson, T. A. 1981, *Ap. J. Suppl.*, **46**, 177.
Boroson, T. A., and Oke, J. B. 1982, *Nature*, in press.
de Vaucouleurs, G. 1948, *Ann. d'Ap.*, **11**, 247.
———. 1953, *M.N.R.A.S.*, **113**, 134.
Freeman, K. C. 1970, *Ap. J.*, **160**, 811.
Green, R. F., and Schmidt, M. 1982, in preparation.
Green, R. F., Williams, T. B., and Morton, D. C. 1978, *Ap. J.*, **226**, 729.
Hawkins, M. R. S. 1978, *M.N.R.A.S.*, **182**, 361.
Hutchings, J. B., Crampton, D., Campbell, B., Gower, A. C., and Morris, S. C. 1982, *Ap. J.*, **262**, in press.
Hutchings, J. B., Crampton, D., Campbell, B., and Pritchet, C. 1981, *Ap. J.*, **247**, 743.
Kormendy, J. 1977, *Ap. J.*, **218**, 333.
Kristian, J. 1973, *Ap. J. (Letters)*, **179**, L61.
Larson, R. B., and Tinsley, B. M. 1978, *Ap. J.*, **219**, 46.
Malkan, M. A., Margon, B., and Chaisson, E. 1982, preprint.
Matthews, T. A., and Sandage, A. R. 1963, *Ap. J.*, **138**, 30.
Miller, J. S., French, H. B., and Hawley, S. A. 1979, in *Pittsburgh Conference on BL Lac Objects*, ed. A. M. Wolfe (Pittsburgh: University of Pittsburgh), p. 176.
———. 1980, in *IAU Symposium 92, Objects of High Redshift*, ed. G. O. Abell and P. J. E. Peebles (Dordrecht: Reidel), p. 83.
Morton, D. C., Williams, T. B., and Green, R. F. 1978, *Ap. J.*, **219**, 381.
Oke, J. B. 1965*a*, *Ap. J.*, **141**, 6.
———. 1965*b*, *Ann. Rev. Astr. Ap.*, **3**, 23.
Oke, J. B., and Gunn, J. E. 1982, preprint.
Osterbrock, D. E. 1960, *Ap. J.*, **132**, 325.
Richstone, D. O., and Oke, J. B. 1977, *Ap. J.*, **213**, 8.
Sandage, A. R. 1973, *Ap. J.*, **180**, 687.
Sandage, A. R., and Miller, W. C. 1966, *Ap. J.*, **144**, 1238.
Sanders, R. H. 1980, *Ap. J.*, **242**, 931.
Spinrad, H., and Taylor, B. J. 1971, *Ap. J. Suppl.*, **22**, 445.
Stockton, A. 1976, *Ap. J. (Letters)*, **205**, L113.
———. 1982, preprint.
Thuan, T. X., Oke, J. B., and Gunn, J. E. 1975, *Ap. J.*, **201**, 45.

Wampler, E. J., Robinson, L. B., Burbidge, E. M., and Baldwin, J. A. 1975, *Ap. J.* (*Letters*), **198**, L49.
Wyckoff, S., Wehinger, P. A., Gehren, T., Morton, D. C., Boksenberg, A., and Albrecht, R. 1980*a*, *Ap. J.* (*Letters*), **242**, L59.
Wyckoff, S., Wehinger, P. A., Spinrad, H., and Boksenberg, A. 1980*b*, *Ap. J.*, **240**, 25.
Wyckoff, S., Wehinger, P. A., and Gehren, T. 1981, *Ap. J.*, **247**, 750.

TODD A. BOROSON and J. B. OKE: 105–24, California Institute of Technology, Pasadena, CA 91125

RICHARD F. GREEN: Steward Observatory, University of Arizona, Tucson, AZ 85721